

PACS numbers: 32.80.Rm; 52.25.Os; 52.50.Jm
DOI: 10.1070/QE2014v044n12ABEH015514

Numerical simulation of microwave amplification in a plasma channel produced in a gas via multiphoton ionisation by a femtosecond laser pulse

A.V. Bogatskaya, E.A. Volkova, A.M. Popov

Abstract. **This paper examines the evolution of a nonequilibrium plasma channel produced in xenon by a femtosecond KrF laser pulse. We demonstrate that such a channel can be used to amplify microwave pulses over times of the order of the relaxation time of the photoelectron energy spectrum in xenon. Using the slowly varying amplitude approximation, we analyse the propagation and amplification of an rf pulse in a plasma channel, in particular when the rf field influences the electron energy distribution function in the plasma.**

Keywords: *plasma channel, amplification of electromagnetic radiation, electron energy distribution function.*

1. Introduction

The formation of extended ionised channels in gases as a result of multiphoton ionisation by intense laser pulses is of considerable interest for a number of practical applications. Of special note are the generation of attosecond VUV and soft X-ray pulses [1, 2], remote atmospheric sensing [3], laser triggering and guiding of high-voltage discharges [4 – 7] and microwave guiding over macroscopically large distances [8, 9]. In particular, Zvorykin et al. [9, 10] presented a theoretical analysis and described an experimental implementation of a sliding-mode plasma waveguide, which enabled microwave signal (λ = 8 mm) transfer to at least 60 m through a 5-cm-radius waveguide with an electron concentration $n_e \sim 10^{12}$ cm^{-3} in the plasma wall.

An important feature of the plasma resulting from gas ionisation by an ultrashort laser pulse is that it is in a highly nonequilibrium state, which may play a very important role in analysis of the above processes. The energy spectrum of photoelectrons produced by multiphoton ionisation of a gas at a pulse duration comparable to the average electron – atom collision time or shorter is known to comprise a number of peaks, each corresponding to the absorption of a particular number of photons. Such an electron energy distribution function (EEDF) is characterised by the presence of energy intervals with an inverted population of electronic states in a continuum, which can be used to amplify electromagnetic radiation in an ionised gas [11]. The possibility of using a plasma channel produced in xenon by an intense femtosecond KrF excimer laser ($\hbar\Omega$ = 5 eV) pulse for amplifying rf pulses was discussed in Ref. [12]. Analysis of the feasibility of amplifying electromagnetic radiation of the subterahertz frequency range in various atomic and molecular gases [12, 13] showed that a xenon plasma as a gain medium has a number of advantages over both molecular gases (nitrogen and air) and other rare gases.

In this paper, based on a joint self-consistent numerical integration of the wave equation in the slowly varying amplitude approximation and Boltzmann's kinetic equation for the EEDF, we examine the propagation of an rf pulse of the subterahertz frequency range through a plasma channel produced in xenon by a femtosecond KrF laser pulse. We analyse conditions under which an rf pulse can be amplified in the nonequilibrium plasma of the channel and evaluate the efficiency of laser pulse energy conversion to energy in the subterahertz frequency range.

A.V. Bogatskaya, A.M. Popov Department of Physics, M.V. Lomonosov Moscow State University, Vorob'evy gory, 119991 Moscow, Russia; D.V. Skobeltsyn Institute of Nuclear Physics, M.V. Lomonosov Moscow State University, Vorob'evy gory, 119991 Moscow, Russia; P.N. Lebedev Physics Institute, Russian Academy of Sciences, Leninsky prosp. 53, 119991 Moscow, Russia; e-mail: alexander.m.popov@gmail.com;
E.A. Volkova D.V. Skobeltsyn Institute of Nuclear Physics, M.V. Lomonosov Moscow State University, Vorob'evy gory, 119991 Moscow, Russia

Received 8 April 2014; revision received 3 June 2014
Kvantovaya Elektronika **44** (12) 1091 – 1098 (2014)
Translated by O.M. Tsarev

2. Kinetics of electrons in a plasma channel produced by an ultrashort laser pulse

When analysing the evolution of the EEDF in a plasma channel produced by a femtosecond laser pulse, it is important to take into consideration that free electrons result only from the multiphoton ionisation of atoms or molecules, whereas avalanche ionisation can be neglected. Moreover, at pulse durations $\tau_p \sim 100$ fs elastic collisions of electrons with atoms (molecules) of the medium can also be neglected. Indeed, the characteristic time of elastic electron – atom collisions in a gas at atmospheric pressure and room temperature ($T \approx 0.03$ eV) can be estimated as $\tau_c \approx 1/(N\sigma v)$, where $N \approx 2.5\times10^{19}$ cm^{-3} is the atomic concentration; $\sigma \sim 10^{-15}$ cm^2 is the elastic electron – atom scattering cross section; and $v \sim 10^8$ cm s^{-1} is a characteristic velocity of electrons resulting from the multiphoton ionisation of the gas. Under the conditions in question, $\tau_c \sim 4\times10^{-13}$ s, which exceeds the laser pulse duration. As pointed out previously [12, 13], in such a situation the EEDF at the end of a laser pulse comprises a number of above-threshold ionisation peaks, and the time evolution of the EEDF as a result of elastic and inelastic collisions with atoms of the medium and electron – electron collisions occurs after the end of the laser pulse.

In the case of a KrF laser beam intensity of $\sim10^{10}$ to 10^{12} W cm^{-2}, xenon atom ionisation is possible as a three-

photon process, whereas the above-threshold ionisation peaks corresponding to the absorption of four, five or more photons can be neglected. In this intensity range, we can also neglect the ac Stark shift of the ground state and continuum states. This means that the initial EEDF can be represented as a peak of energy $\varepsilon_0 = 3\hbar\Omega - I_i$ (where $I_i \approx 12.13$ eV is the ionisation potential of the xenon atom) and width $\Delta\varepsilon$, determined by the spectral width of the laser pulse. In the intensity range under consideration and at a pulse duration $\tau_p \sim 100$ fs, the degree of ionisation of the forming plasma can be estimated as $\alpha = n_e/N \approx 10^{-9}$ to 10^{-5} [14], where n_e is the electron concentration.

In analysing the time evolution of the EEDF, we will assume, like in a previous study [12], that a laser pulse in a gas produces an ionised channel with a radial electron concentration distribution and a highly nonequilibrium EEDF corresponding to electron generation as a consequence of the three-photon ionisation of xenon atoms. It is convenient to represent such a distribution by a Gaussian:

$$n(\varepsilon, t=0) = \frac{1}{\Delta\varepsilon\sqrt{\pi\varepsilon}} \exp\left[-\frac{(\varepsilon-\varepsilon_0)^2}{\Delta\varepsilon^2}\right]. \quad (1)$$

The value of $\Delta\varepsilon$ is determined by the spectral width of the laser pulse and is ~0.2 eV in the case of a transform-limited pulse of duration ~50–100 fs. The above-threshold ionisation peaks can then be neglected.

The distribution function (1) satisfies the normalisation condition

$$\int_0^\infty n(\varepsilon, t=0)\sqrt{\varepsilon}\,\mathrm{d}\varepsilon = 1, \quad (2)$$

and $n(\varepsilon, t)\sqrt{\varepsilon}$ is the probability density of finding an electron of energy ε.

The time evolution of the EEDF can be assessed by solving Boltzmann's kinetic equation. In moderately strong fields, where the electron velocity distribution is only slightly anisotropic, it is convenient to analyse Boltzmann's equation in the two-term approximation. This approximation was examined in detail previously [15, 16] (see also [17] and references therein). Given that the EEDF is influenced by the field of an rf wave propagating in the plasma, the equation in question can be written in the form

$$\frac{\partial n(\varepsilon,t)}{\partial t}\sqrt{\varepsilon} = \frac{\partial}{\partial\varepsilon}\left[\frac{e^2E_0^2\nu_{tr}(\varepsilon)}{3m(\omega^2+\nu_{tr}^2)}\varepsilon^{3/2}\frac{\partial n}{\partial\varepsilon}\right]$$
$$+ \frac{2m}{M}\frac{\partial}{\partial\varepsilon}\left\{\nu_{tr}(\varepsilon)\varepsilon^{3/2}\left[n(\varepsilon,t) + T\frac{\partial n(\varepsilon,t)}{\partial\varepsilon}\right]\right\}$$
$$+ Q^*(n) + Q_{ee}(n). \quad (3)$$

Here, E_0 is the field amplitude of the rf wave (of frequency ω) propagating in the plasma; $T \approx 0.03$ eV is the gas temperature; m is the electron mass; M is the mass of the xenon atom; and $\nu_{tr} = N\sigma_{tr}(\varepsilon)\sqrt{2\varepsilon/m}$ and $\sigma_{tr}(\varepsilon)$ are the transport frequency and transport scattering cross section. The term $Q^*(n)$ represents inelastic collisions of electrons with xenon atoms and is of negligible importance under the conditions below. The term $Q_{ee}(n)$ represents electron–electron collisions and was examined in detail previously [15]. The effect of electron–electron collisions on the evolution of the EEDF reduces to a faster maxwellisation and was analysed in greater detail elsewhere [13]. In particular, this effect was shown to be essential starting at an electron concentration $n_e = 10^{12}$ cm^{-3}, i.e. at a degree of ionisation $\alpha \approx 4\times10^{-8}$.

Equation (3) is a diffusion equation in energy space, with the diffusion coefficient determined by both the gas temperature and the term representing electron–electron collisions [15]. It is important to note that the effect of an external field of frequency ω on the EEDF can also be described in a diffusion approximation, so a sufficiently strong electric field of a wave propagating in a plasma will also contribute to the diffusion broadening of the photoelectron peak.

Equation (3) subject to the initial condition (1) was solved numerically using an implicit scheme, in the energy range $\varepsilon = 0$–10 eV. The integration time and energy steps, δt and $\delta\varepsilon$, were 10^{-13} s and 10^{-2} eV. The cross sections of elementary processes in xenon were taken from Hayashi [18, 19]. The transport scattering cross section of xenon is presented in Fig. 1a. Its characteristic features are the Ramsauer minimum and a region at energies from 0.64 to 5.0 eV where the cross section rapidly increases with energy. It is these features of the transport scattering cross section that are responsible for the possibility of amplifying rf radiation in a photoionised plasma [12].

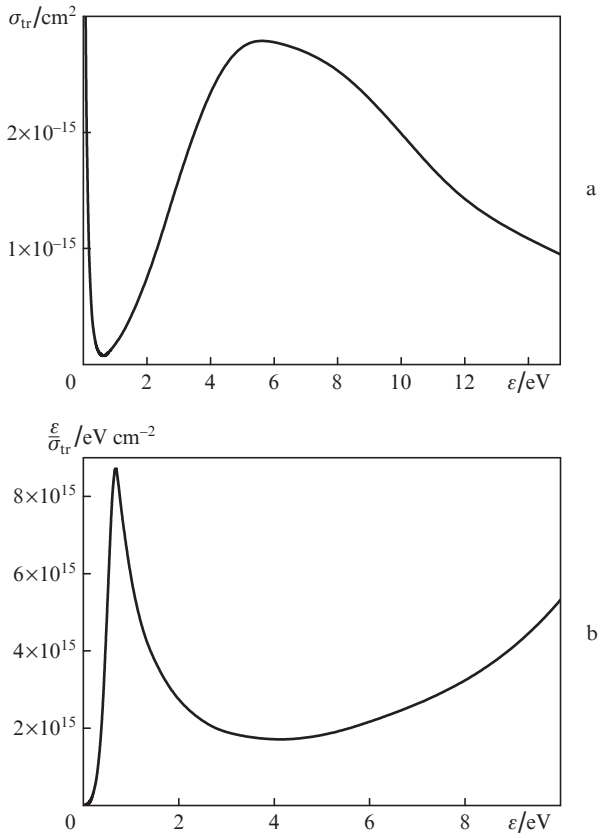

Figure 1. (a) Transport cross section for electron scattering by xenon atoms; (b) plot of $\varepsilon/\varepsilon_{tr}$ against ε.

The EEDF obtained by numerically solving Eqn (3) was used to calculate the electrodynamic characteristics of the plasma channel produced by a laser pulse. In particular, the complex conductivity of the plasma at frequency ω, $\sigma_\omega = \sigma'_\omega + i\sigma''_\omega$, can be written in the form [11, 15]

$$\sigma_\omega = \frac{2}{3}\frac{e^2 n_e}{m}\int_0^\infty \frac{\varepsilon^{3/2}[\nu_{tr}(\varepsilon)+i\omega]}{\omega^2+\nu_{tr}^2(\varepsilon)}\left[-\frac{\partial n(\varepsilon,t)}{\partial\varepsilon}\right]d\varepsilon. \quad (4)$$

The real part of this expression describes the energy dissipation of an electromagnetic wave in the plasma. The absorption coefficient for radiation of frequency ω is given by

$$\mu_\omega = \frac{4\pi\sigma'_\omega}{c} = \frac{1}{3}\frac{\omega_p^2}{c}\int_0^\infty \frac{\varepsilon^{3/2}\nu_{tr}(\varepsilon)}{\omega^2+\nu_{tr}^2(\varepsilon)}\left[-\frac{\partial n(\varepsilon,t)}{\partial\varepsilon}\right]d\varepsilon, \quad (5)$$

where $\omega_p^2 = 4\pi e^2 n_e/m$ is the square of the plasma frequency of the electron gas.

As pointed out previously [11, 12], the integral in (5) for the peak structure of the EEDF, which essentially means population inversion in a continuum, may be negative when the condition $\omega < \nu_{tr}$ is satisfied. In such a situation, the medium will be capable of amplifying electromagnetic radiation. As shown earlier [12, 13], the amplification condition for a photoionised plasma in xenon is satisfied in the case of rf radiation with $\omega \leqslant 10^{12}$ s^{-1} if the photoionisation peak is located in the region where the transport cross section increases with energy and if, at the same time, the condition

$$\frac{d}{d\varepsilon}\frac{\varepsilon}{\sigma_{tr}(\varepsilon)} < 0 \quad (6)$$

is satisfied, i.e. the transport cross section should be a superlinear function of energy. Condition (6) is satisfied for xenon atoms in the energy range ~1–3 eV (Fig. 1b).

If changes in the electron energy spectrum are only due to elastic collisions of electrons with neutral atoms, the characteristic EEDF relaxation time can be estimated as

$$\tau_\varepsilon \approx \frac{M}{2m}\frac{1}{\nu_{tr}}, \quad (7)$$

which gives $\tau_\varepsilon \approx 10^{-7}$ s. This means that it is over such times that one would expect amplification of electromagnetic radiation in a plasma. Therefore, a plasma channel produced in xenon by a femtosecond KrF laser beam will be able to amplify rf pulses (with frequencies up to the terahertz range) several tens of nanoseconds in duration.

Formula (7) takes into account only the electron energy loss in elastic electron–atom collisions. At the same time, electron–electron collisions lead to a faster maxwellisation of the photoelectron spectrum and, as a consequence, to zero gain. Estimates and numerical simulation results [13] demonstrate that, even at an electron concentration $n_e = 10^{12}$ cm^{-3}, taking into account electron–electron collisions has a significant effect on the evolution of the EEDF. At $n_e = 10^{13}$ cm^{-3}, maxwellisation of the spectrum takes ~200 ns. Calculations indicate that, in effect, electron–electron collisions considerably increase

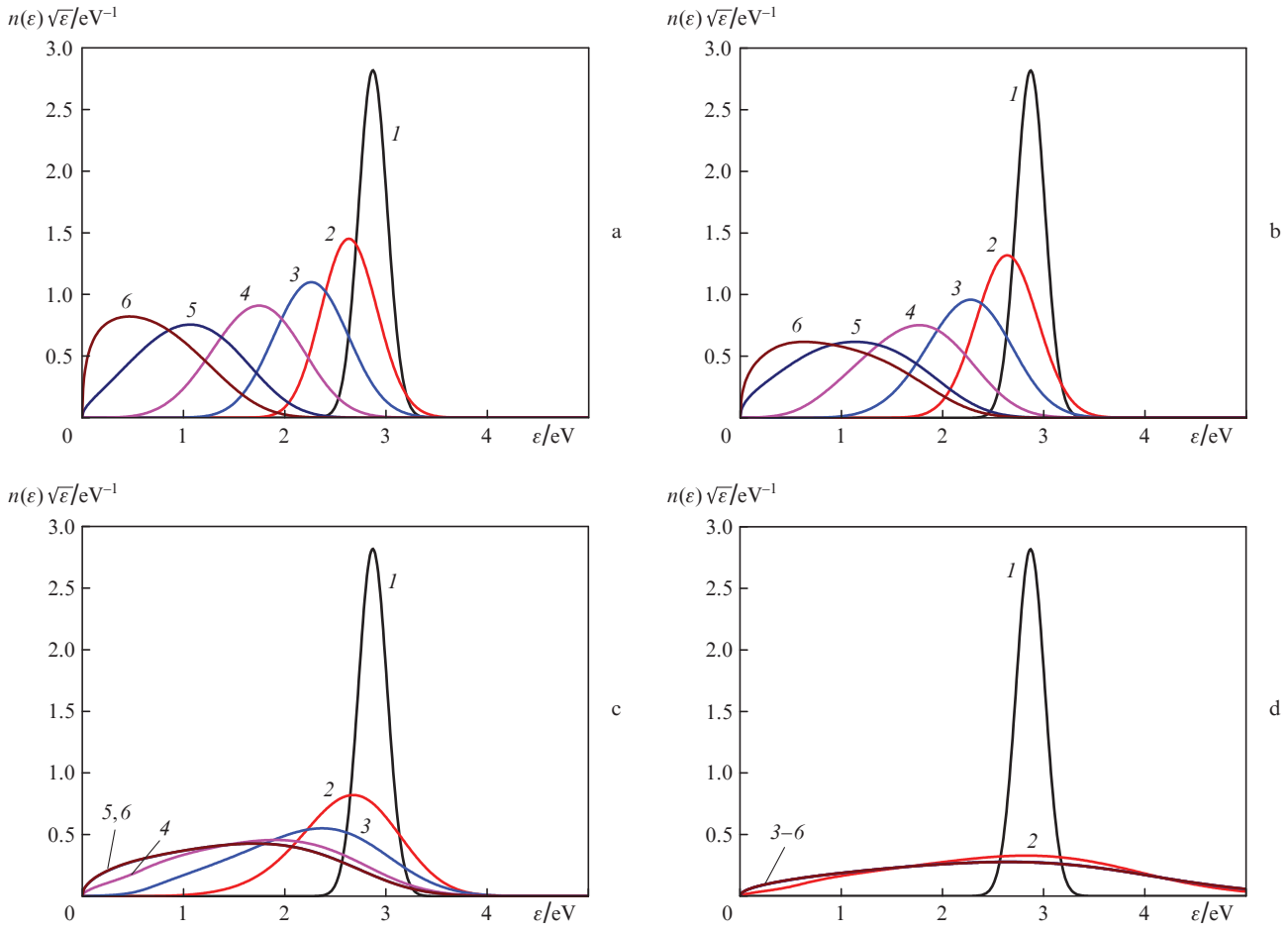

Figure 2. EEDF in a xenon plasma at times t = (*1*) 0, (*2*) 3, (*3*) 10, (*4*) 30, (*5*) 100 and (*6*) 200 ns after plasma channel formation at rf field intensities of (a) 0, (b) 10, (c) 100 and (d) 10^3 W cm^{-2}. Electron concentration $n_e = 3\times10^{12}$ cm^{-3}.

the electron diffusion coefficient in energy space, leading to a rapid broadening of the photoelectron peak and, as a consequence, to a rapid decrease in the time interval during which the gain coefficient in the channel is positive.

In the above analysis of the evolution of the energy spectrum of photoelectrons in a plasma channel, the radiation being amplified was assumed to be weak and have no effect on the EEDF. Clearly, this is justified when the electron energy diffusion coefficient related to the field being amplified is smaller than the energy diffusion coefficients related to elastic collisions of electrons with gas atoms (molecules) and electron–electron collisions. Estimating the electron energy diffusion coefficient related to rf radiation in the plasma (for $\omega \ll \nu_{tr}$) as $D_\omega \sim e^2E_0^2\varepsilon/(3m\nu_{tr})$, we find that the above reasoning is correct if

$$\frac{e^2E_0^2}{3m\nu_{tr}} \ll \max\left\{\frac{2m}{M}T\nu_{tr}, \langle\varepsilon\rangle\nu_{ee}\right\}, \qquad (8)$$

where $\langle\varepsilon\rangle$ is the spectrum-averaged electron energy and ν_{ee} is the electron–electron collision frequency. For example, in the case of xenon atoms, $\langle\varepsilon\rangle \approx 2$ eV, $T \approx 0.03$ eV and an electron concentration $n_e = 3\times10^{12}$ cm^{-3}, condition (8) is satisfied at rf field intensities far below 1 kW cm^{-2}.

The above estimates are supported by numerical calculation results. Figure 2 shows EEDFs in a xenon plasma at different instants in time for cases where the initial energy distribution (1) relaxes in the presence of an rf field ($\omega \approx 5\times10^{11}$ s^{-1}) of various intensities. It is seen that, indeed, the field markedly accelerates the diffusion broadening of the photoelectron peak: the EEDF relaxation to a steady state takes ~100 ns at an rf field intensity of 100 W cm^{-2} and just 10 ns at an intensity of 1 kW cm^{-2}.

As pointed out above, the diffusion broadening of the photoelectron peak reduces the ability of a plasma channel to amplify rf radiation. Indeed, the gain coefficients $k_\omega = -\mu_\omega$ calculated for various radiation intensities at a frequency $\omega = 5\times10^{11}$ s^{-1} (Fig. 3) demonstrate that the time interval during which k_ω is positive decreases from 20 to 2 ns as the intensity increases from zero to 1 kW cm^{-2}. At a radiation intensity of 10 kW cm^{-2}, the plasma channel retains amplifying properties for just 0.1 ns. This means that the intensity of microwave pulses up to 2 ns in duration can be amplified to ~1 kW cm^{-2}. Note also that the amplification of an electromagnetic wave in a plasma suggests that taking into account the effect of the field being amplified on the EEDF in the plasma channel leads to a reduction in electron energy in it, i.e., in the conditions under consideration, the electric field of an rf wave leads to cooling of the electron component of the plasma. Indeed, the data presented in Fig. 4 demonstrate that taking into account the effect of rf radiation leads to faster plasma cooling in the initial stage of EEDF relaxation.

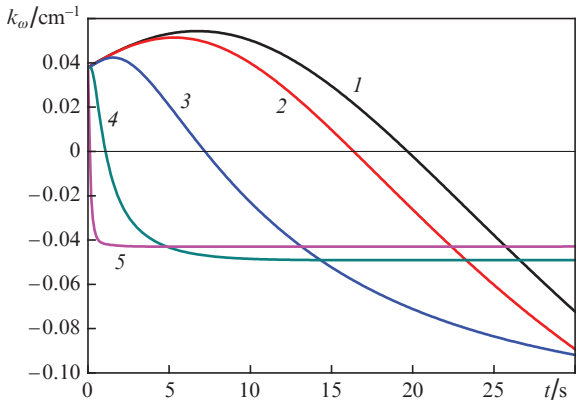

Figure 3. Time dependences of the gain coefficient for electromagnetic radiation in a plasma channel in xenon at radiation intensities of (*1*) 0, (*2*) 10, (*3*) 100, (*4*) 10^3 and (*5*) 10^4 W cm^{-2}. Negative values correspond to electromagnetic radiation absorption in the plasma. The calculations were performed for an electron concentration $n_e = 3\times10^{12}$ cm^{-3}.

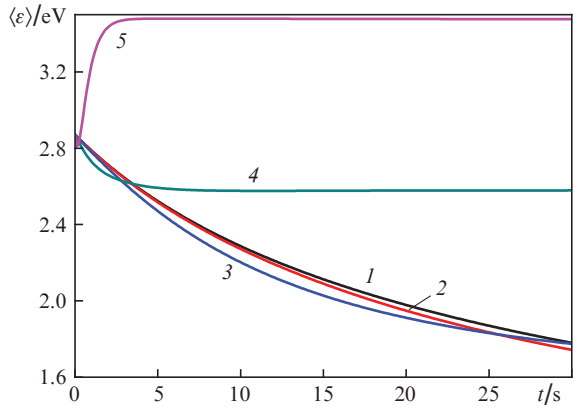

Figure 4. Time dependences of the spectrum-averaged photoelectron energy in a xenon plasma at rf field intensities of (*1*) 0, (*2*) 10, (*3*) 100, (*4*) 10^3 and (*5*) 10^4 W cm^{-2}.

In particular, in the intensity range 0–100 W cm^{-2} the spectrum-averaged electron energy decreases with increasing intensity in the time interval 20–25 ns. At an intensity of 1 kW cm^{-2}, faster electron cooling is only observed within ~3 ns. Subsequently, the average electron energy plateaus at ~2.6 eV. By contrast, an rf field of intensity 10 kW cm^{-2} heats the electron gas: its average energy increases from its initial value of 2.87 eV to ~3.5 eV in just 2–3 ns.

It is worth pointing out that, physically, the effect under consideration – amplification of electromagnetic radiation in a highly nonequilibrium plasma – is similar to the negative absolute conductivity of a gas discharge plasma in a dc electric field, which was predicted by Rochlenko [20] and Shizga and McMahon [21] and discussed in detail in a number of publications [22–24]. A negative absolute conductivity of a plasma is a kinetic effect that leads to the formation of an electron flow opposite in direction to the force acting on each electron. In such a situation, the electrons, on average, give up their energy to the field of the electromagnetic wave, thereby ensuring amplification.

3. Propagation of rf pulses in a plasma channel

In this section, jointly solving the wave equation and Boltzmann's kinetic equation we examine the propagation and amplification of an rf pulse in a plasma channel produced in xenon by a femtosecond KrF laser pulse. The propagation of electromagnetic radiation in a medium can be described by the following wave equation:

$$\nabla^2\boldsymbol{E} - \frac{1}{c^2}\frac{\partial^2\boldsymbol{E}}{\partial t^2} = \frac{4\pi}{c^2}\frac{\partial\boldsymbol{j}}{\partial t}. \qquad (9)$$

Here, $\boldsymbol{E}$ is the electric field of the wave and $\boldsymbol{j}$ is the current density in the plasma, which is eventually determined from Boltzmann's kinetic equation. The rf field is taken to be linearly polarised (along the x axis) and to propagate along the z axis.

In numerical analysis of Eqn (9), we employ the slowly varying amplitude (SVA) approximation [25]. In this approximation, the electric field of an rf pulse propagating along the z axis, $E(\boldsymbol{r}, z, t)$, can be represented in the form

$$E(\boldsymbol{r}, z, t) = E_0(\rho, z, t)\exp[\mathrm{i}(kz - \omega t)], \tag{10}$$

and the electric current through the plasma, with negligible dispersion, is then given by

$$j(\rho, z, t) = \sigma_\omega(\rho, z, t)\, E_0(\rho, z, t)\exp[\mathrm{i}(kz - \omega t)]. \tag{11}$$

Here, E_0 is the rf pulse envelope; k is the wavenumber, $\omega = 5\times10^{11}$ s^{-1}; and ρ is a transverse coordinate. In what follows, the electron concentration in the plasma channel is taken to be sufficiently low ($n_e \leqslant 10^{13}$ cm^{-3}), so that the pulse propagates through the channel at the speed of light. Therefore, $k = \omega/c$. In addition, the conductivity of the plasma is taken to be a slowly varying function of time and spatial coordinate, i.e. $|\mathrm{d}\sigma_\omega/\mathrm{d}t| \ll \omega|\sigma_\omega|$ and $|\nabla\sigma_\omega| \ll k|\sigma_\omega|$. The following expression can then be obtained for the envelope of the rf pulse:

$$\mathrm{i}k\left(\frac{\partial E_0}{\partial z} + \frac{1}{c}\frac{\partial E_0}{\partial t}\right) = -\frac{1}{2}\nabla_\perp^2 E_0 + \frac{\mathrm{i}}{2}\, k_\omega(\rho, z, t) k E_0, \tag{12}$$

where $k_\omega(\rho, z, t)$ is the spatiotemporal distribution of the gain coefficient for electromagnetic radiation in the plasma and $\nabla_\perp^2$ is the transverse Laplace operator. The first term on the right-hand side of (12) describes the diffraction divergence of the electromagnetic pulse and the second term represents its amplification (absorption) in the plasma.

If the rf field is relatively weak and has no effect on the EEDF relaxation process in the plasma (in the conditions under consideration, this is so at intensities $I < 10$ W cm^{-2}), Eqn (12) is linear and should be solved for a preset distribution of the gain coefficient $k_\omega(\rho, z, t)$, which can be found from the EEDF obtained by numerically integrating Boltzmann's equation. In contrast, if the rf field has a significant effect on the EEDF in at least some regions of space, Eqn (12) should be solved self-consistently with Boltzmann's equation for the EEDF at every spatial point.

It follows from the above analysis of the EEDF relaxation process that the amplification time τ_a in the plasma channel may range from several nanoseconds to 15–20 ns, depending on the intensity of the pulse being amplified. For this reason, a femtosecond laser pulse propagating in a gas produces a spatial trail – an amplification region several tens of centimetres in length, $c\tau_a$ (Fig. 5). To ensure the most efficient amplification of an rf pulse in such a situation, it is convenient to create conditions under which pulses travel through the medium one after another, so that an rf pulse is constantly in the amplification zone produced by a laser pulse.

To numerically integrate Eqn (12), it is convenient to introduce new variables: $\zeta = z$ and $\tau = t - z/c$ (retarded time). Given that both pulses travel at the speed of light, i.e. $k_\omega(\rho, z, t) = k_\omega(\rho, t - z/c) = k_\omega(\rho, \tau)$, Eqn (12) can be rewritten in the form

$$\mathrm{i}k\frac{\partial E_0(\rho, \zeta, \tau)}{\partial \zeta} = -\frac{1}{2}\nabla_\perp^2 E_0 + \frac{\mathrm{i}}{2}k k_\omega(\rho, \tau)\, E_0(\rho, \zeta, \tau). \tag{13}$$

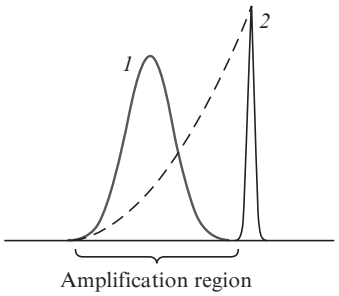

Figure 5. Spatial structure of (*1*) rf and (*2*) laser pulses at some instant in time. The dashed curve shows the spatial gain coefficient profile.

Equation (13) was solved numerically using the finite-element method in a spatial region of dimensions $0 \leqslant \rho \leqslant \rho_{max} = 40$ cm and $0 \leqslant \zeta \leqslant z_{max} = 100$ cm. The total simulation time did not exceed $t_{max} = z_{max}/c \approx 3.3$ ns, which corresponded to laser pulse propagation over a distance z_{max}. As boundary conditions, the electric field was taken to be zero on the distant boundaries $\rho = \rho_{max}$ and $\zeta = z_{max}$. At $\zeta = 0$, we set the temporal profile of the rf pulse:

$$E_0(\rho, \zeta = 0, \tau = t) = AR(\rho)\sin^2(\pi t/\tau_p), \tag{14}$$

where A is the amplitude of the rf pulse on the axis ($\rho = 0$) and $R(\rho)$ is the radial electric field distribution function. Subsequently, the pulse was taken to consist of 50 field periods, i.e. at $\omega = 5\times10^{11}$ s^{-1} the pulse duration was $\tau_p \approx 0.628$ ns and the function $R(\rho)$ was represented by a Gaussoid:

$$R(\rho) = \exp[-\rho^2/(2\rho_f^2)], \tag{15}$$

where ρ_f is the rf beam radius. The radial electron concentration profile produced by a KrF laser pulse, which determines the gain (absorption) coefficient, was also taken to be Gaussian:

$$n_e(\rho) = n_e(\rho = 0)\exp[-\rho^2/(2\rho_e^2)], \tag{16}$$

where $n_e(\rho = 0)$ is the electron concentration in the centre of the plasma channel and ρ_e is its width.

The integration time and coordinate steps were $\delta t = \tau_p/512$, $\delta z = c\delta t$ and $\delta\rho = \rho_{max}/640$. The gain coefficient was determined at each spatial point with coordinates ρ and ζ by integrating Boltzmann's equation.

Consider first the results obtained by numerically integrating the wave equation (13) subject to the boundary condition (14) in the weak-field regime, where the effect of the rf pulse on the EEDF in the plasma channel can be neglected. Figure 6 shows the intensity profiles $I = cE_0^2(\rho, \zeta, \tau)/(8\pi)$ for an initial beam radius $\rho_f = 2$ cm and a plasma channel radius $\rho_e = 1$ cm at variable τ ($\rho = 0$) and ρ ($\tau = \tau_p/2$, which corresponds to the maximum in the initial pulse envelope). The first profile can be viewed, for example, as the temporal pulse envelope at different fixed values of z or as a distribution with respect to the z coordinate at fixed instants in time. The point $\tau = 0$, or $z = ct$, corresponds to the leading edge of the propagating pulse, and the coordinate $\tau = \tau_p$ corresponds to its trailing edge. The spatial extent of the pulse, $c\tau_p$, is then $\sim$1.9 cm. In the case under consideration, the gain coefficient is $k_\omega \approx 0.04$ cm^{-1} and can be thought to be constant during the entire period of pulse propagation (Fig. 3). In the absence

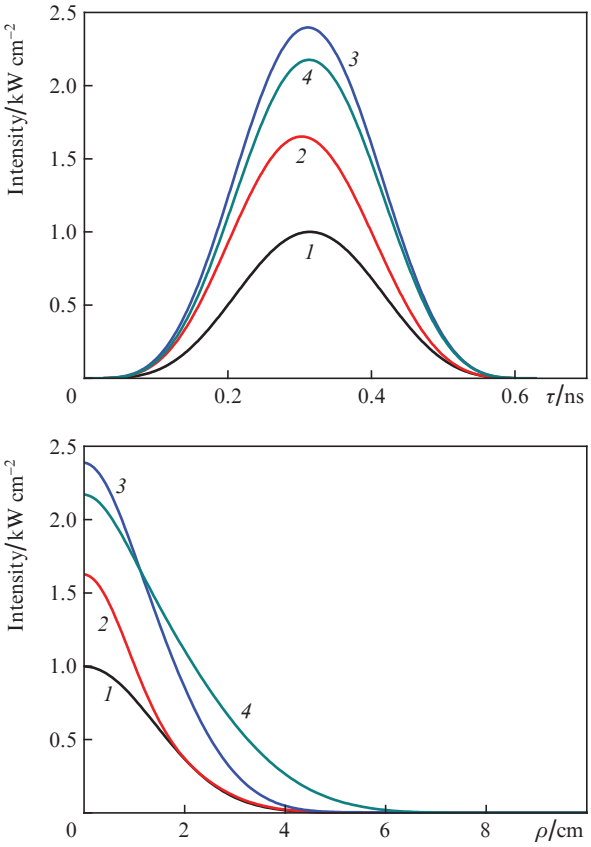

Figure 6. Spatiotemporal structure of a microwave pulse with an initial peak intensity of 1 W cm^{-2} at propagation lengths in the medium L = (*1*) 0, (*2*) 18.3, (*3*) 55.2 and (*4*) 92.1 cm. The plasma channel radius is ρ_e = 1 cm.

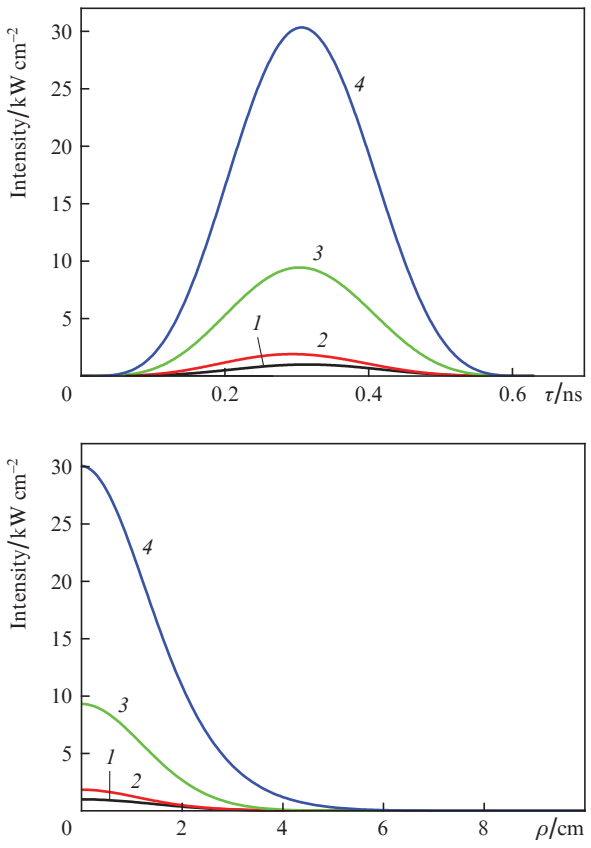

Figure 7. Same as in Fig. 6 but for a plasma channel radius ρ_e = 2 cm.

of diffraction divergence, this would lead to an increase in intensity by about 40 times over a length L = 92.1 cm. However, the diffraction length corresponding to the radius of the beam being amplified is $L_d = k\rho_e^2 \approx 17$ cm. As a result, at propagation lengths $L > L_d$ the peak intensity first grows more slowly and then decreases because of the diffraction broadening of the beam.

Figure 7 presents results of analogous calculations of the spatiotemporal structure of an rf pulse at a larger plasma channel radius (ρ_e = 2 cm). In this case, the diffraction length is $L_d \approx 70$ cm, so the pulse propagates almost without diffraction over distances of ~100 cm, and its intensity increases by $I(L)/I_0 \approx 30$ times over a length L = 92.1 cm.

There is special interest in the case where a pulse has a relatively high initial intensity and thus has a significant effect on the evolution of the EEDF in the plasma channel in the amplification process. Results of such calculations for an initial radiation intensity I_0 = 1 kW cm^{-2} are presented in Fig. 8. It is seen that, over the same propagation length L = 92.1 cm, the peak intensity of an rf pulse increases by just a factor of 9.5. This is accompanied by marked distortion of the pulse shape, because its leading edge is amplified stronger. At distances $L > 90$ cm, the central and trailing parts of the laser pulse are in a region where the signal is absorbed as a result of changes in the EEDF, which leads to a reduction in pulse duration and an increase in the spectral width of the pulse.

The above is confirmed as well by the τ dependences of the gain (absorption) coefficient on the channel axis, calculated from the EEDF by jointly solving the wave equation

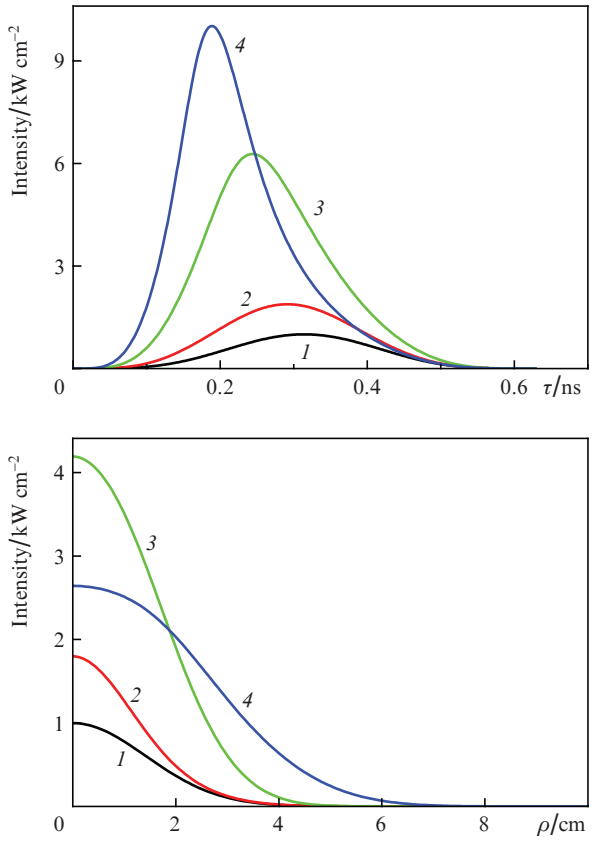

Figure 8. Same as in Fig. 7 but for a pulse with an initial peak intensity of 1 kW cm^{-2}.

and Boltzmann's kinetic equation (Fig. 9). It is seen in Fig. 9 that the signal amplification zone constantly narrows down, so that at $L \approx 100$ cm most of the pulse is in the absorption region. Subsequently, in such a situation the pulse duration decreases rapidly, which places significant limitations on the possibility of describing the pulse propagation process in terms of the SVA approximation.

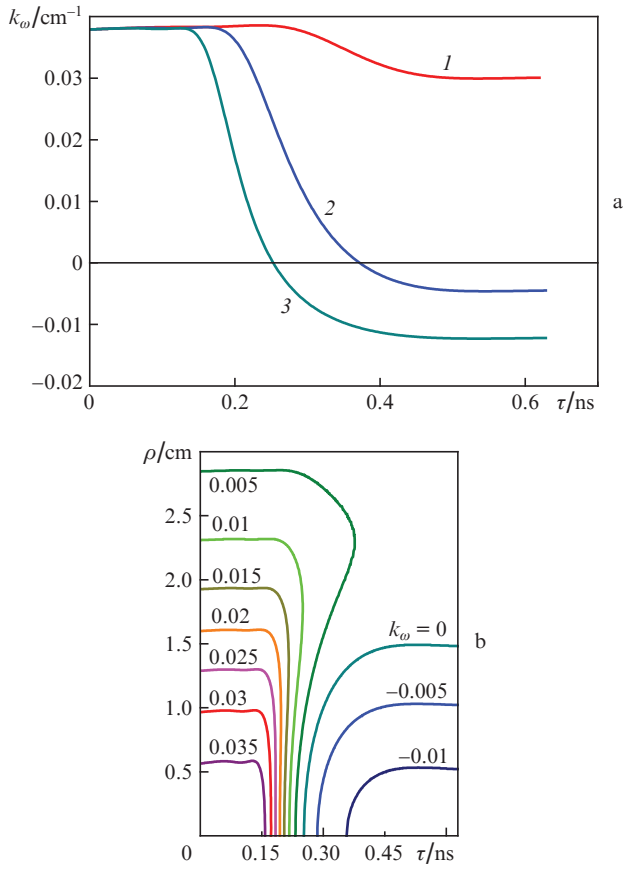

Figure 9. Gain (absorption) coefficient for microwave electromagnetic radiation in a plasma channel in xenon: (a) distributions along the channel axis at propagation lengths in the medium L = (*1*) 18.3, (*2*) 55.2 and (*3*) 92.1 cm; (b) two-dimensional distribution in the form of contour plots for L = 92.1 cm. The initial peak intensity is I_0 = 1 kW cm^{-2} and the plasma channel radius is ρ_e = 2 cm. Negative values correspond to absorption of electromagnetic radiation in the plasma.

Our calculations make it possible to estimate the efficiency of KrF laser pulse energy conversion to rf energy. Indeed, the laser energy needed to ionise a xenon atom is $3\hbar\omega$ = 15 eV. Therefore, at a propagation length $L \approx 100$ cm and photoelectron concentration $n_e = 3\times10^{12}$ cm^{-3}, the energy deposited in the medium is $\sim7\times10^{-4}$ J cm^{-2}. On the other hand, the initial energy of a pulse with a peak intensity of 1 kW cm^{-2} is $\sim5\times10^{-7}$ J cm^{-2}, and the pulse energy increases by almost one order of magnitude over a length of 100 cm. This means that, in the conditions under consideration, ~1% of the energy deposited in the plasma during gas photoionisation is then converted to microwave energy. Note that the energy conversion efficiency can be increased, in particular by increasing the spatial dimensions of the plasma channel.

Note also that, from a practical point of view, it may be of interest to examine the case where a plasma channel is produced not via multiphoton gas ionisation but via the single-photon ionisation of easily ionasable impurities. A laser pulse producing a plasma channel may then have a relatively low intensity, but the ionisation potential of the impurity should be chosen such that the corresponding photoionisation peak lies in the desired energy range.

4. Conclusions

The present results demonstrate that a nonequilibrium plasma channel produced in xenon by a femtosecond KrF laser pulse can be used to amplify rf pulses having a carrier frequency in the subterahertz frequency range. An appreciable gain can be achieved when such pulses travel through the medium one after another, so that an rf pulse is constantly in the amplification zone produced by a laser pulse.

Acknowledgements. This work was supported by the Russian Foundation for Basic Research (Grant No. 12-02-00064). A.V. Bogatskaya acknowledges the support from the Dynasty Nonprofit Foundation (Support Programme for Students in the Field of Theoretical Physics); the Education and Research Centre, P.N. Lebedev Physics Institute, Russian Academy of Sciences; and the Russian Academy of Sciences (Support to Young Scientists Programme). The numerical simulations were performed on the Chebyshev SKIF supercomputer, M.V. Lomonosov Moscow State University.

References

1. Agostini P., DiMauro L.F. *Rep. Prog. Phys.*, **67**, 813 (2004).
2. Krausz F., Ivanov M. *Rev. Mod. Phys.*, **81**, 163 (2009).
3. Penano J., Sprangle P., Hafizi B., Gordon D., Fernsler R., Scully M. *J. Appl. Phys.*, **111**, 033105 (2012).
4. Zhao X.M., Wang Y.C., Diels J.-C., Elizondo J. *IEEE J. Quantum Electron.*, **31**, 599 (1995).
5. Tzortzakis S., Franco M.A., André Y.-B., Chiron A., Lamouroux B., Prade B.S., Mysyrowicz A. *Phys. Rev. E*, **60**, R3505 (1999).
6. Rodriguez M., Sauerbrey R., Wille H., Wöste L., Fujii T., André Y.-B., Mysyrowicz A., Klingbeil L., Rethmeier K., Kalkner W., Kasparian J., Salmon E., Yu J., Wolf J.-P. *Opt. Lett.*, **27**, 772 (2002).
7. Ionin A.A., Kudryashov S.V., Levchenko A.O., Seleznev L.V., Shutov A.V., Sinitsyn D.V., Smetanin I.V., Ustinovsky N.N., Zvorykin V.D. *Appl. Phys. Lett.*, **100**, 104105 (2012).
8. Châteauneuf M., Payeur S., Dubois J., Kieffer J.-C. *Appl. Phys. Lett.*, **92**, 091104 (2008).
9. Zvorykin V.D., Levchenko A.O., Smetanin I.V., Ustinovskii N.N. *Pis'ma Zh. Eksp. Teor. Fiz.*, **91**, 226 (2010).
10. Zvorykin V.D., Levchenko A.O., Shutov A.V., Solomina E.V., Ustinovsky N.N., Smetanin I.V. *Phys. Plasmas*, **19**, 033509 (2012).
11. Bunkin F.V., Kazakov A.E., Fedorov M.V. *Usp. Fiz. Nauk*, **107**, 559 (1972).
12. Bogatskaya A.V., Popov A.M. *Pis'ma Zh. Eksp. Teor. Fiz.*, **97**, 453 (2013) [*JETP Lett.*, **97**, 388 (2013)].
13. Bogatskaya A.V., Volkova E.A., Popov A.M. *Kvantovaya Elektron.*, **43**, 1110 (2013) [*Quantum Electron.*, **43**, 1110 (2013)].
14. Delone N.B., Krainov V.P. *Multiphoton Processes in Atoms* (Berlin: Springer-Verlag, 1994).
15. Ginzburg V.L., Gurevich A.V. *Usp. Fiz. Nauk*, **70**, 201 (1960).
16. Raizer Yu.P. *Laser-Induced Discharge Phenomena* (New York: Consultants Bureau, 1977; Moscow: Nauka, 1974).
17. Popov A.M., Rakhimov A.T., Rakhimova T.V. *Plasma Phys. Rep.*, **19**, 651 (1993).
18. Hayashi M. *J. Phys. D*, **16**, 581 (1983).
19. Hayashi M. *Bibliography of Electron and Photon Cross-Sections with Atoms and Molecules Published in the 20th Century: Xenon, Technical Report NIFS-DATA-79* (Toki-shi, Japan, National Institute for Fusion Research, 2003).

20. Rokhlenko A.V. *Zh. Eksp. Teor. Fiz*., **75**, 1315 (1978).
21. Shizga S., McMahon D.R.A. *Phys. Rev. A*, **32**, 3669 (1985).
22. Aleksandrov N.L., Napartovich A.P. *Usp. Fiz. Nauk*, **163**, 1 (1993).
23. Dyatko N.A. *J. Phys. Conf. Ser.*, **71**, 012005 (2007).
24. Kudryavtsev A.A., Smirnov A.S., Tsendin L.D. *Fizika tleyushchego razryada* (Glow Discharge Physics) (St. Petersburg: Lan', 2010) Ch. 3, Sect. 3.7.2.
25. Akhmanov S.A., Nikitin S.Yu. *Physical Optics* (Oxford: Clarendon, 1997; Moscow: Mosk. Gos. Univ., 1998) Part 4.